Soft Matter



PAPER



Cite this: Soft Matter, 2023, **19**, 497

Received 2nd December 2022, Accepted 14th December 2022

DOI: 10.1039/d2sm01578a

rsc.li/soft-matter-journal

Fluorescent azobenzene-confined coiled-coil mesofibers*

Kamia Punia,‡a Dustin Britton,‡a Katharina Hüll, bc Liming Yin,a Yifei Wang,a P. Douglas Renfrew, M. Lane Gilchrist, Richard Bonneau, Dirk Trauner 10 and Jin K. Montclare ** **abf

Fluorescent protein biomaterials have important applications such as bioimaging in pharmacological studies. Self-assembly of proteins, especially into fibrils, is known to produce fluorescence in the blue band. Capable of self-assembly into nanofibers, we have shown we can modulate its aggregation into mesofibers by encapsulation of a small hydrophobic molecule. Conversely, azobenzenes are hydrophobic small molecules that are virtually non-fluorescent in solution due to their highly efficient photoisomerization. However, they demonstrate fluorogenic properties upon confinement in nanoscale assemblies by reducing the non-radiative photoisomerization. Here, we report the fluorescence of a hybrid protein-small molecule system in which azobenzene is confined in our protein assembly leading to fiber thickening and increased fluorescence. We show our engineered protein Q encapsulates AzoCholine, bearing a photoswitchable azobenzene moiety, in the hydrophobic pore to produce fluorescent mesofibers. This study further investigates the photocontrol of protein conformation as well as fluorescence of an azobenze-containing biomaterial.

Introduction

Azobenzenes generally do not exhibit fluorescence in solution owing to their fast trans-cis isomerization that leads to nonradiative relaxation of the excited state. 1 Nevertheless, there are some exceptions where azobenzenes are known to fluoresce. In these cases, chromophores are confined in densely packed structures such as bilayers.²⁻⁴ Shimomura et al. first reported fluorescence emission from azobenzenes confined in a bilayer structure.4 Enhanced fluorescence has also been observed from azobenzene-containing polymeric micelles and vesicles.⁵⁻⁹ Bo and co-workers have further shown that micellization provides a significant enhancement of fluorescence from azobenzene

containing diblock copolymers. 10 This increase in fluorescence intensity upon micellar entrapment is also accompanied by a reduction in the rate of isomerization of trans-azobenzene. Illumination of the micelles with UV light leads to irreversible decrease in fluorescence due to dissociation of the micelles. In contrast, Dong et al. have demonstrated reversible, visible light-driven fluorescence behaviour from azobenzene containing polymeric vesicles.11 The vesicles result in pH-responsive fluorescence emission from polymer micelles covalently conjugated to azobenzenes achieved by introducing carboxylic acid groups on one of the repeating units. 11 While the fluorescent properties of azobenzenes constricted in polymeric systems have been studied substantially, to the best of our knowledge, their fluorogenicity by confinement in protein assemblies has not been explored.

Chromophore-binding self-assembling proteins have precedent in biological systems.¹² Rhodospin is an example present in rod cells of the retina, comprised of seven transmembrane helices that assemble to form a retinal chromophore-binding pocket. 11-cis-retinal chromophore acts as an inverse agonist that photoisomerizes into all-trans state when bound to rhodospin, triggering cascade of events in visual signal transduction.¹² Recently, we have reported an azobenzene molecule AzoCholine, a photoswitchable agonist for nicotinic acetylcholine receptors.¹³ The change in geometry of AzoCholine upon absorption of photon provides optical control of the biological activity of dorsal root ganglion and hippocampal neurons.

^a Departments of Chemical and Biomolecular Engineering, Biomedical Engineering, NYU Tandon School of Engineering, Brooklyn, New York 11201, USA. E-mail: montclare@nyu.edu

^b Department of Chemistry, New York University, New York, New York 10003, USA

^c Department of Chemistry, Ludwig Maximilian University, München, Germany

 $^{^{}d}$ Center for Genomics and Systems Biology, Department of Biology, New York University New York, New York 10003, USA

^e Department of Chemical Engineering and Biomedical Engineering, The City College of the City University of New York, New York, New York 10031, USA

^fDepartment of Biomaterials, NYU College of Dentistry, New York, NY, 10010, USA

g Department of Chemistry, University of Pennsylvania, Philadelphia, PA 19104, USA

^h Center for Computational Biology, Flatiron Institute, New York, NY 10010, USA

[†] Electronic supplementary information (ESI) available. See DOI: https://doi.org/ 10.1039/d2sm01578a

[‡] Authors contributed equally.

Soft Matter **Paper**

Akin to other azobenzenes, AzoCholine is an inherently nonfluorescent molecule in solution.

Here, we investigate the fluorogenicity of AzoCholine by encapsulating it in the hydrophobic binding pore of our previously reported coiled-coil protein, Q. A homopentameric assembly, Q further self-assembles into robust nanofibers ranging up to hundreds of nanometers in diameter and with the ability to bind small hydrophobic molecules.¹⁴ Q, like other collagen derivatives, undergoes supramolecular assembly upon binding the hydrophobic small molecule curcumin (CCM). We similarly discover the ability for AzoCholine to induce mesofibril assembly upon binding to Q. We investigate the selfassembly and conformation of Q upon AzoCholine binding and the effect of AzoCholine photoisomerization. The result is a fluorescent mesoscale fiber with photoresponsive changes in both protein conformation and nanofibril organization. The present work on self-assembly of proteins with photoresponsive behaviour of azobenzene-containing biomaterials will potentially have broad applications as a fluorescent probe and as a model platform for investigating the cascade of photo-controlled events in biological systems including rhodopsin.

Results and discussion

The binding of AzoCholine with Q was performed under dark conditions to achieve incorporation of the trans-isomer. Transmission electron micrographs (TEM) were obtained to confirm the fiber assembly of Q. Using increasing molar ratios of Q: AzoCholine, we note an increase and plateau at a 1.5 Q:AzoCholine ratio (Fig. S2b, ESI†). As reported in our previous work, 14 protofibril bundling was observed in the case of Q. The electrostatic surface charge distribution in Q allowed for both lateral and longitudinal assembly of protofibrils to form nanofibers with 100.48 \pm 37.79 nm in diameter (Fig. 1a). Scanning electron micrography (SEM) and TEM were used to study the assembly of AzoCholine-bound Q protein. Binding of AzoCholine into the hydrophobic pore of Q led to the formation of robust microfibers with average diameter of 13.73 \pm 7.42 μm observed from SEM micrographs (Fig. 1b). A subpopulation of protein aggregates of nanoscale dimensions was also observed when AzoCholine-bound Q protein was imaged with TEM (Fig. 1c). The ratio of microfibers to the nanoaggregates could not be determined due to the use of different instruments for imaging the two populations.

To confirm that microfiber aggregation was not influenced by the addition of DMSO, widefield microscopy and SEM were used at 1.5 Q:AzoCholine molar ratios in which microfibers were absent micrographs (Fig. S3a and b, ESI†). Previously, similar drug binding studies have been completed with the hydrophobic small molecule, curcumin (CCM). 15 CCM is known to induce fiber thickening in collagen and Q. 14,16,17 We hypothesize that a similar mechanism occurs between AzoCholine and Q where binding of AzoCholine causes exposure of nonpolar groups and increased surface activity in Q, which further drives its fiber aggregation.

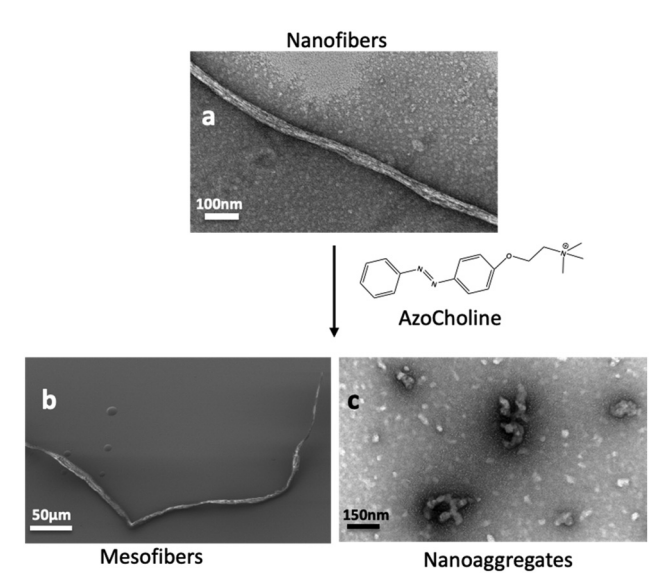


Fig. 1 Self-assembly of Q protein pre- and post-AzoCholine binding. (a) TEM image illustrating the nanoscale assembly of Q protein prior to AzoCholine encapsulation and the transition to (b) micron scale protein fibers by SEM and (c) nanoaggregates upon AzoCholine binding as observed in bottom TEM image.

The fast-relaxing photochromic ligand, AzoCholine does not display fluorescence emission in solution. Rapid isomerization of excited azobenzes leads to their non-radiative relaxation, which in turn leads to fluorescence quenching. Successful encapsulation of AzoCholine into the promiscuous binding pocket of Q generates fluorescent mesofibers, termed as Qazo fibers. We hypothesize that preventing the main relaxation event allows excited trans azobenenes to return to the ground state via fluorescence emission. Restricting the molecule in a confined geometry impedes the non-radiative relaxation process producing fluorescence. We also note that increased fluorescence may be the result of changes in nanofibril organization and fiber thickening since it has been previously found that fibril formation of protein aggregates provides a band in the blue product, 18 similar to trans-AzoCholine. To explore the behaviour, we demonstrate that AzoCholine bound samples provide added fluorescence after dialysis of free AzoCholine (Fig. S2a, ESI†). Interestingly, prior to dialysis we observe that AzoCholine provides significant fluorescence quenching, a previously noted property of azobenzenes. 19,20 We further confirm the entrapment is associated primarily with the hydrophobic binding pocket by comparing binding conditions in the presence and absence of 100 µM NiCl₂ (Fig. S2b, ESI†) which we have previously shown to destroy the self-assembly of Q.21 We note that addition of NiCl2 reduces fluorescence of Qazo and Q significantly, suggesting it promotes disassembly of both Q and Q nanofibers. We confirm that the fluorescence of Qazo samples after addition of NiCl₂ is the result of nanoagregates where ordered nanofibers were absent from TEM images (Fig. S4, ESI†) in agreement with TEM images of Q alone after addition of NiCl2 seen previously.21

Confocal microscopy of Qazo fibers was conducted with an AIRYSCAN detector; a representative 3D reconstruction shows Soft Matter **Paper**

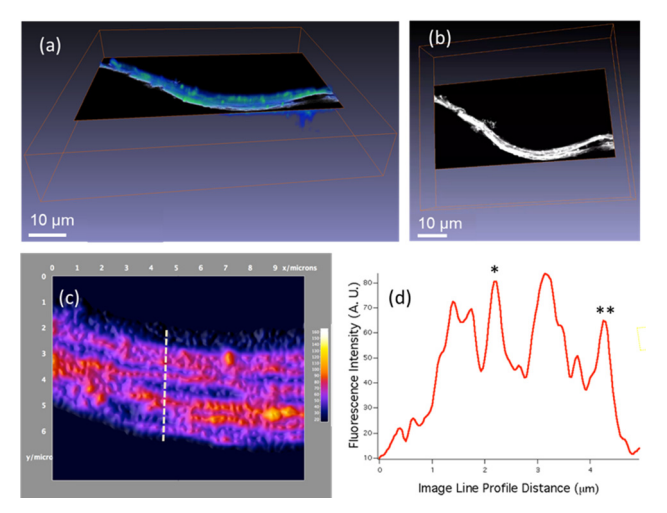


Fig. 2 Representative 3D reconstruction of a Qazo protein fiber obtained with the AIRYSCAN super-resolution method. (a) 3D Volren representation of the Q fiber showing an XY orthogonal view and shown at a different angle in (b) at scale bar widths of 10 µm. (c) Shows a zoomed-in Z-section as a false color image obtained from the dotted R.O.I. in the cross section shown in (b). (d) Was taken from the image line profile indicated in panel (c). The width of the Q fiber at this point is $\sim 3.41 \, \mu m$, with the single fiber widths for the fibers labeled * and ** at 250 and 240 nm, respectively (from FWHM).

uniform distribution of AzoCholine along the mesofiber (Fig. 2). Fluorescent Qazo fibers have an average diameter of $27.56 \pm 6.16 \,\mu m$. Lower average fiber diameters in SEM is likely attributed to dehydration of samples prior to obtaining electron micrographs.

To compare the binding interactions of AzoCholine conformers with the protein, Rosetta Macromolecular Modeling Suite²² has been employed to perform small-molecule docking simulations (Fig. 3). The internal cavity of the Q-bundle varies in width. The widest part of this cavity is a pentalobular void formed near the N-terminus of the helices as a result of a small kink of the helix induced by PRO26 and the short ALA25 side chain. This portion of the cavity is capable of accommodating both cis and trans conformations of the azobenzene moiety of the AzoCholine molecule. Analysis of the best scoring models

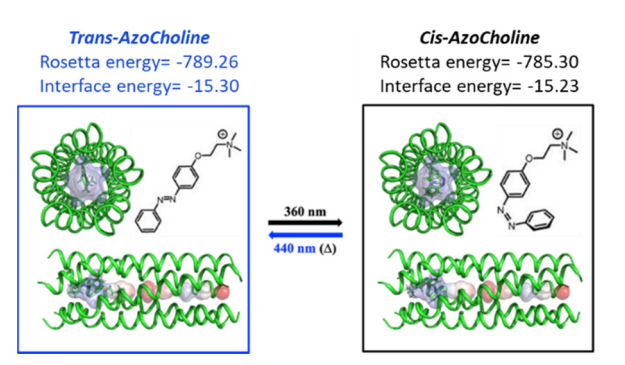


Fig. 3 Binding interactions of AzoCholine isomers with the protein Q. The lowest-energy models from docking simulations illustrating binding of trans and cis isomers of AzoCholine by the Q protein.

show the central phenyl ring of the AzoCholine intercalating into one of the lobes of the large void. All low energy models present the choline moiety in a full extended conformation, and the best scoring models have the positively charged trimethylamine group of the ligand occupying a slightly negatively charged cavity toward the C-terminus of the helices. Both cis and trans conformation of the ligand can be accommodated without deformations of the backbone; C-alpha RMSD between docked and undocked conformations is less than 0.1 angstroms. However, binding of the trans conformation is energetically more favourable as indicated by the lower total energy and interface energy.

The effect of photoisomerization on the fluorescence of Qazo fibers is examined by illuminating the mesofibers with 370 nm UV light for trans to cis isomerization of the azobenzene moiety and switching it back from cis to trans state by using 460 nm blue light. An irreversible decrease of 33.2% in fluorescence of the fibers (n = 5) is observed after three photoisomerization cycles of AzoCholine (Fig. 4). The decrease in fluorescence can be attributed to the change in hydrophobic/hydrophilic balance due to an increase in the dipole moment of azobenzene upon its trans to cis photoisomerization.4 In some studies, isomerization of azobenzenes has been shown to affect the morphology of the azobenzene containing polymer micelles that could even lead to their dissociation.5 Thus, the decrease in fluorescence intensity of azobenzene can also be due to change in morphology of the protein upon photoisomerization, which in turn may cause AzoCholine to be expelled out. Similarly, the decrease in trans-AzoCholines may result in a decrease in fluorescence due to a decrease in mesofiber content that is stabilized by the *trans*-AzoCholines bound to the hydrophobic pocket of Q.

UV/Vis absorbance spectra are monitored to examine the effect of binding to Q protein and photoswitching on the characteristic bands of AzoCholine (Fig. S1, ESI†). To separate the supernatant comprising nm scale protein aggregates (Fig. 1c) and the pellet containing mesofibers (Fig. 1b), Qazo is centrifuged at 2000 \times g for 5 min. The supernatant is next illuminated for 200 s each with three alternate cycles of 370 nm and 460 nm

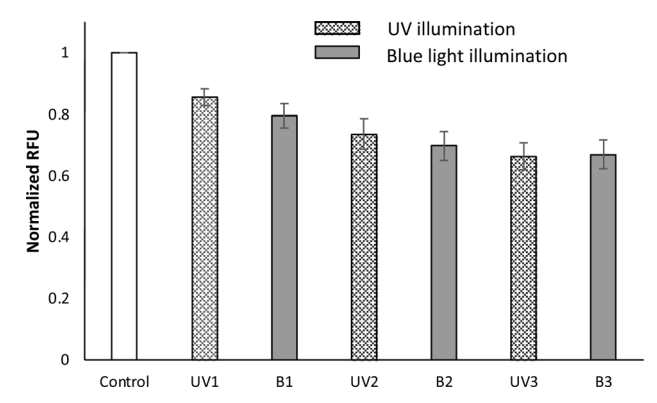


Fig. 4 Effect of photoisomerization on the fluorescence of Qazo mesofibers. Fluorescence intensity measurements of Qazo fibers after each 10 minutes of illumination with 370 nm UV and 460 nm blue light. Results shown are the average of five independent trials.

Paper Soft Matter

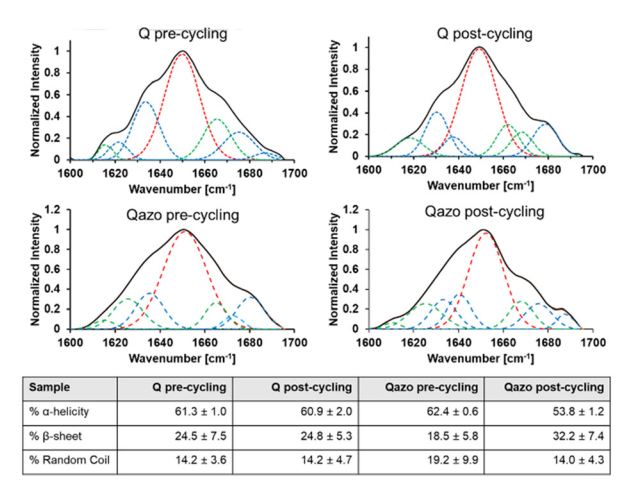


Fig. 5 Secondary structure analyses. ATR-FTIR spectra acquired for Q and Qazo pre- and post-photoisomerization cycles. Table below shows secondary structure content for Q and Qazo pre- and post-photoisomerization cycles by ATR-FTIR peak deconvolution – α -helical peak (red), β-sheet peak (blue), random coil (green). Results shown are the average of three independent trials.

light. Absorbance spectra are obtained in the dark and after each period of illumination, showing the characteristic change in intensity of the π – π * band. The sample is turbid during the switching and a baseline-shift of the absorbance spectrum after the photoisomerization cycles indicates precipitation. We confirm an increase in nanoaggregates after photoisomerization cycles in TEM images (Fig. S5, ESI†). This suggests that indeed isomerization of the azobenzene photoswitch affects the aggregation of the protein, as previously hypothesized, causing reduced lateral assembly into mesofibers and reduction of confined *trans*-AzoCholine.

The effect of photoisomerization on the secondary structure of Q and Qazo protein samples were investigated by ATR-FTIR prior to and after three alternate cycles with 370 nm and 460 nm illumination. After deconvolution of spectra, we observe 61.3 \pm 1.0% and 62.4 \pm 0.6% α -helical content for Q and Q-AzoCholine fibers, respectively (Fig. 5). Hence, the protein retains α -helical structure even after macromolecular assembly of fibers. Upon illumination with UV and blue light, unbound Q does not show any considerable change in α -helical, β -sheet, or random coil content whereas Qazo exhibits a statistically significant (p-value = 0.004) decrease of 8.6% in α -helicity when compared to the samples prior to photoisomerization. Notably this α -helical loss is complemented by an increase from 18.5% to 32.2% β-sheet content and a decrease from 19.2% to 14% random coil content. The FTIR results further suggest that photoisomerization of AzoCholine-bound to Q affects the morphology of the protein that triggers the release of AzoCholine.

Covalent introduction of photoisomerizable groups has previously provided the ability to photo-control the activity of a protein by regulating its α -helicity. The Woolley group has synthesized a short peptide comprising two cysteine residues that are crosslinked by an azobenzene molecule allowing the photoregulation of helical content. ²³ trans to cis

photoisomerization leads to a significant increase in helicity due to a better match of the *cis*-crosslinker length with the spacing of the i, i + 7 residues of an ideal α -helix. *trans* to *cis* photoisomerization of an azobenzene linker between i, i + 4 cysteine residues has also been reported to cause a marked increase in helicity whereas in position i, i + 11, the helix content decreases significantly.²⁴

Efforts have been made previously to introduce azobenzene moieties in proteins to investigate azobenzene-mediated photoregulation of protein function, whereas there are no attempts to demonstrate the fluorogenicity of azobenzene upon binding to proteins.^{25,26} Incorporation of azobenzenes in proteins has mainly been performed by three approaches including site-selective incorporation of unnatural azobenzene amino acids, 25,27 bio-orthogonal conjugation, 28 and inclusion of cysteine-reactive ligands. 29,30 Our study has demonstrated the first approach of introducing azobenzene in proteins via non-covalent interactions to explore its fluorogenicity and ability to modulate protein function by photoregulation. Non-covalent encapsulation of the azobenzene moiety into our protein system causes restriction, rapid isomerization of AzoCholine, and fiber aggregation which produces fluorescent fibers and an emission maximum in the blue band. Fluorogencity of Qazo complements previous work on fluorogen activating proteins (FAPs) where rapid movement of non-fluorescent small molecules are constricted leading to their subsequent fluorescence activation. 31,32 These two-component protein/fluorogen probes do not fluoresce until the protein is bound to the fluorogen, making them great alternative candidates to traditional fluorescent proteins for imaging living systems.

Conclusions

In summary, we have investigated the fluorescence of Qazo fibers as the result of organization into mesofibers with confined trans-AzoCholines. Confocal-microscopy images of Qazo fibers illustrate uniform fluorescence due to ordered aggregation and confinement of AzoCholine. Fluorescent binding studies indicate that addition of AzoCholine indeed produces increased fluorescence. We attribute this both to the characteristic increase in intensity in the blue band from increased fibrilization (nano-to-mesoscale fibers) and confinement of trans-AzoCholine. Confinement of trans-AzoCholine is confirmed by small-molecule docking simulations that suggest that the binding interactions of AzoCholine conformers with protein Q is energetically more favourable in the trans-state producing a positive interaction in the pore resulting in transformation into fluorescent mesofibers. A significant decrease in the fluorescence of Qazo fibers is observed upon subjecting them to three cycles of photoisomerization of AzoCholine. The helical content of the protein can be photoregulated by incorporation of an azobenzene moiety in the pore of the α -helical structure. The ability to photoregulate the fluorescence and helical content can provide a wide-range of applications including generation of light-activated self-assembling proteins for photopharmacological studies.

Soft Matter **Paper**

Conflicts of interest

There are no conflicts to declare.

Acknowledgements

This work was supported by NSF-DMREF under Award Number DMR 1728858, and NSF-MRSEC Program under Award Number DMR 1420073.

References

- 1 H. Rau, Angew. Chem., Int. Ed. Engl., 1973, 12, 224-235.
- 2 Y. Li, N. Zhou, W. Zhang, F. Zhang, J. Zhu, Z. Zhang, Z. Cheng, Y. Tu and X. Zhu, J. Polym. Sci., Part A: Polym. Chem., 2011, 49, 4911-4920.
- 3 K. Tsuda, G. C. Dol, T. Gensch, J. Hofkens, L. Latterini, J. W. Weener, E. W. Meijer and F. C. DeSchryver, J. Am. Chem. Soc., 2000, 122, 3445-3452.
- 4 M. Shimomura and T. Kunitake, J. Am. Chem. Soc., 1987, **109**, 5175-5183.
- 5 G. Wang, X. Tong and Y. Zhao, Macromolecules, 2004, 37, 8911-8917.
- 6 E. Blasco, J. d Barrio, C. Sánchez-Somolinos, M. Piñol and L. Oriol, Polym. Chem., 2013, 4, 2246-2254.
- 7 H. Ren, D. Chen, Y. Shi, H. Yu and Z. Fu, *Polymer*, 2016, 97, 533-542.
- 8 J. Xu, W. Zhang, N. Zhou, J. Zhu, Z. Cheng, Y. Xu and X. Zhu, J. Polym. Sci., Part A: Polym. Chem., 2008, 46, 5652-5662.
- 9 Y. Xiang, X. Xue, J. Zhu, Z. Zhang, W. Zhang, N. Zhou and X. Zhu, Polym. Chem., 2010, 1, 1453-1458.
- 10 Q. Bo and Y. Zhao, Langmuir, 2007, 23, 5746-5751.
- 11 R. Dong, B. Zhu, Y. Zhou, D. Yan and X. Zhu, *Polym. Chem.*, 2013, 4, 912-915.
- 12 T. P. Sakmar and T. Huber, in Encycl. Neurosci., ed. L. R. Squire, Academic Press, Oxford, 2009, pp. 365-372.
- 13 A. Damijonaitis, J. Broichhagen, T. Urushima, K. Hull, J. Nagpal, L. Laprell, M. Schonberger, D. H. Woodmansee, A. Rafiq, M. P. Sumser, W. Kummer, A. Gottschalk and D. Trauner, ACS Chem. Neurosci., 2015, 6, 701-707.
- 14 J. Hume, J. Sun, R. Jacquet, P. D. Renfrew, J. A. Martin, R. Bonneau, M. L. Gilchrist and J. K. Montclare, Biomacromolecules, 2014, 15, 3503-3510.

- 15 D. Britton, J. Monkovic, S. Jia, C. Liu, F. Mahmoudinobar, M. Meleties, P. D. Renfrew, R. Bonneau and J. K. Montclare, Biomacromolecules, 2022, 23, 4851-4859.
- 16 N. Nishad Fathima, R. Saranya Devi, K. B. Rekha and A. Dhathathreyan, J. Chem. Sci., 2009, 121, 509-514.
- 17 N. N. Fathima, A. Dhathathreyan and T. Ramasami, *J. Chem.* Sci., 2010, 122, 881-889.
- 18 C. S. H. Jesus, H. T. Soares, A. P. Piedade, L. Cortes and C. Serpa, Analyst, 2021, 146, 2383-2391.
- 19 M. Autret, M. Le Plouzennec, C. Moinet and G. Simonneaux, J. Chem. Soc., Chem. Commun., 1994, 1169-1170.
- 20 L. S. Runtsch, D. M. Barber, P. Mayer, M. Groll, D. Trauner and J. Broichhagen, Beilstein J. Org. Chem., 2015, 11, 1129-1135.
- 21 H. T. More, K. S. Zhang, N. Srivastava, J. A. Frezzo and J. K. Montclare, Biomacromolecules, 2015, 16, 1210-1217.
- 22 A. Leaver-Fay, M. Tyka, S. M. Lewis, O. F. Lange, J. Thompson, R. Jacak, K. Kaufman, P. D. Renfrew, C. A. Smith, W. Sheffler, I. W. Davis, S. Cooper, A. Treuille, D. J. Mandell, F. Richter, Y.-E. A. Ban, S. J. Fleishman, J. E. Corn, D. E. Kim, S. Lyskov, M. Berrondo, S. Mentzer, Z. Popović, J. J. Havranek, J. Karanicolas, R. Das, J. Meiler, T. Kortemme, J. J. Gray, B. Kuhlman, D. Baker and P. Bradley, Methods Enzymol., 2011, 487, 545-574.
- 23 J. R. Kumita, O. S. Smart and G. A. Woolley, Proc. Natl. Acad. Sci. U. S. A., 2000, 97, 3803-3808.
- 24 D. G. Flint, J. R. Kumita, O. S. Smart and G. A. Woolley, Chem. Biol., 2002, 9, 391-397.
- 25 M. Bose, D. Groff, J. Xie, E. Brustad and P. G. Schultz, J. Am. Chem. Soc., 2006, 128, 388-389.
- 26 A. A. John, C. P. Ramil, Y. Tian, G. Cheng and Q. Lin, Org. Lett., 2015, 17, 6258-6261.
- 27 C. Hoppmann, V. K. Lacey, G. V. Louie, J. Wei, J. P. Noel and L. Wang, Angew. Chem., Int. Ed., 2014, 53, 3932-3936.
- 28 Y.-H. Tsai, S. Essig, J. R. James, K. Lang and J. W. Chin, Nat. Chem., 2015, 7, 554-561.
- 29 E. Bartels, N. H. Wassermann and B. F. Erlanger, Proc. Natl. Acad. Sci. U. S. A., 1971, 68, 1820-1823.
- 30 M. Banghart, K. Borges, E. Isacoff, D. Trauner and R. H. Kramer, Nat. Neurosci., 2004, 7, 1381-1386.
- 31 S. Xu and H.-Y. Hu, Acta Pharm. Sin. B, 2018, 8, 339-348.
- 32 A. S. Klymchenko, Acc. Chem. Res., 2017, 50, 366-375.